

A slip model for micro/nano gas flows induced by body forces

Quy-Dong To, C. Bercegeay, Guy Lauriat, Céline Léonard, Guy Bonnet

▶ **To cite this version:**

Quy-Dong To, C. Bercegeay, Guy Lauriat, Céline Léonard, Guy Bonnet. A slip model for micro/nano gas flows induced by body forces. Microfluidics and Nanofluidics, 2010, 8 (3), pp.417-422. 10.1007/s10404-009-0532-4 . hal-00714817

HAL Id: hal-00714817
https://hal.science/hal-00714817

Submitted on 7 Mar 2016

HAL is a multi-disciplinary open access archive for the deposit and dissemination of scientific research documents, whether they are published or not. The documents may come from teaching and research institutions in France or abroad, or from public or private research centers.

L'archive ouverte pluridisciplinaire **HAL**, est destinée au dépôt et à la diffusion de documents scientifiques de niveau recherche, publiés ou non, émanant des établissements d'enseignement et de recherche français ou étrangers, des laboratoires publics ou privés.

A slip model for micro/nano gas flows induced by body forces

Q. D. To · C. Bercegeay · G. Lauriat · C. Léonard · G. Bonnet

Abstract A slip model for gas flows in micro/nano-channels induced by external body forces is derived based on Maxwell's collision theory between gas molecules and the wall. The model modifies the relationship between slip velocity and velocity gradient at the walls by introducing a new parameter in addition to the classic Tangential Momentum Accommodation Coefficient. Three-dimensional Molecular Dynamics simulations of helium gas flows under uniform body force field between copper flat walls with different channel height are used to validate the model and to determine this new parameter.

Keywords Rarefied effect · Kinetic Maxwell model · External volume force · Slip model · Tangential Momentum Accommodation Coefficient · MD simulation

List of symbols

λ	Mean free path
H, B, L	Channel height, width and length
Kn	Knudsen number
n, ρ	Number density, mass density
d	Molecular diameter
L_s, L^*_s	Slip length, dimensionless slip length
x, y, z	Cartesian coordinate
$\hat{z}$	Normalized coordinate
σ_v	Tangential Momentum Accommodation Coefficient
v, $\hat{v}$	Tangential velocity, normalized tangential velocity
v_{slip}, $\hat{v}_{\text{slip}}$	Slip velocity, normalized slip velocity
v_{ref}	Reference velocity
$N^{\pm}$	Molecules going upward N^+ and downward N^- with respect to the control surface s
N	Total number of molecules passing through s
$<v_x^{\pm}>$	Average velocity of molecules going upward $<v_x^+>$ and downward $<v_x^->$ with respect to s
v_s, v_w	Gas velocity near the wall, velocity of the wall
$<\tau>$, $\bar{c}$	Mean collision time, thermal speed
k_B, T	Boltzmann constant, absolute temperature
m, γ_x	Molecular mass, acceleration along x-axis
α, β	Slip parameters of the present model
v_λ	Gas velocity at distance λ from the wall
μ, μ^*, $\bar{\mu}$	Gas viscosity, scaled viscosity, kinetic theoretical viscosity
V_i	Potential energy of atom i
F, ρ_e, ϕ	Potential functions of Embedded Atom Model
σ_{a-b}, ϵ_{a-b}	Parameters of Lennard Jones potential between molecules a and b
r_{ij}	Distance between two molecules i and j

Q. D. To (✉) · C. Bercegeay · G. Lauriat · C. Léonard · G. Bonnet
Université Paris-Est, Laboratoire Modelisation et Simulation Multi Echelle, FRE 3160 CNRS, 5 Boulevard Descartes, 77454 Marne-la-Vallée Cedex 2, France
e-mail: quy-dong.to@univ-paris-est.fr

1 Introduction

The velocity of a fluid close to a solid wall is always different from the wall velocity even if the latter is perfectly diffusive. Especially, when the channel height is decreased to that of MEMS or NEMS devices (Micro/Nano Electro-Mechanical Systems), this phenomenon becomes highly important and must be taken into account. The Knudsen number Kn, the ratio between the mean free path λ and the

characteristic length of the channel H, is the relevant parameter to quantify the slip effects. The mean free path λ is usually defined as the average distance that molecules travel between collisions and equal to

$$\lambda = \frac{1}{\sqrt{2}n\pi d^2} \tag{1}$$

where n is number density, and d is the effective molecular diameter. According to Maxwell's model (1879), the slip length L_s in continuous fluid mechanics can be determined via the Tangential Momentum Accommodation Coefficient, also denoted by TMAC or σ_v as follows

$$L_s = \frac{2 - \sigma_v}{\sigma_v}\lambda \tag{2}$$

The slip velocity, v_{slip} is calculated by the formula

$$v_{\text{slip}} = L_s \frac{\partial v}{\partial z}\bigg|_w \tag{3}$$

The term, $\frac{\partial v}{\partial z}\big|_w$ is the normal derivatives of the tangential velocity component at the walls, assuming that the normal to the wall is in the z-direction. If the velocity and coordinate in Eq. 3 are scaled with a reference velocity, v_{ref} and the channel height, H, we have

$$\hat{v}_{\text{slip}} = L_s^\star \frac{\partial \hat{v}}{\partial \hat{z}}\bigg|_w, \quad L_s^\star = \frac{L_s}{H} \tag{4}$$

where $\hat{v}_{\text{slip}} = v_{\text{slip}}/v_{\text{ref}}$ and $\hat{z} = z/H$. The term $L_s^\star$ is called the dimensionless slip length and is equal to

$$L_s^\star = \frac{2 - \sigma_v}{\sigma_v}\text{Kn} \tag{5}$$

when the Maxwell model is used. Consequently, for a given accommodation coefficient, Eq. 5 predicts that $L_s^\star$ is proportional to Kn. When Kn tends towards zero, we recover the no slip condition and when Kn increases, the slip effect increases. The Maxwell model is widely used to describe the slip at the walls because it only needs one parameter only, σ_v.

The physical meaning of σ_v in (2,5) is that if M molecules arrive at the wall, $\sigma_v M$ of them are reflected diffusively, and the remaining $(1 - \sigma_v)M$ molecules are reflected specularly. Based on Eq. 2, one can determine TMAC by either experiments or Molecular Dynamics (MD) simulations. Some experimentalists controlled macroscopic quantities such as pressure and mass flow rate and made use of the relationship with the slip velocity to find TMAC (see e.g. Arkilic et al. 2001; Colin et al. 2004). Arkilic et al. (2001) studied flows of nitrogen, argon and carbon dioxide through rectangular silicon channels and found TMAC ranging between 0.75 and 0.85. Colins et al. (2004) worked on the couples silicon–nitrogen and silicon–helium and found a relatively high coefficient, 0.93. Recently, Maali and Bhushan (2008) studied confined air flow between a spherical glass particle glued to the cantilever of an atomic force microscopy (AFM) and a glass plate. They let the cantilever oscillating and measured the hydrodynamic damping factor. As a consequence, a value of the slip length of about 118 nm was obtained. It corresponds to an accommodation coefficient of 0.72. Direct measurements of TMAC on the couple He–Cu by Seidl (see Finger et al. 2007; Gad-el-Hak 1999) stated that the coefficient depends on the collision angle between gas and solid, ranging from 0.6 to 1.0. On the contrary, Cao et al. (2004, 2005, 2006) using MD approaches to simulate flows, revealed that TMAC at Ar–Pt interface can be as small as 0.2 and influenced by temperature and surface roughness. Arya et al. (2003) simulated directly the collisions between gas and wall. Their results showed the dependence of TMAC on the wall's lattice structure. It remains constant as long as the drift velocity is small enough (less than 100 m/s). Finger et al. (2007) used similar method as Arya et al. (2003) to show that TMAC is affected by the adsorbed layer, and their results matched the previous experiment of Seidl on the couple copper-helium. Speaking, in general, both experimental and MD works gave a rather scattering results of TMAC and reflected the dependency of TMAC on many factors. Hence, this coefficient should be understood as an effective one and must be used with caution.

Extensions of Maxwell's model to different configurations have been considered in the past. When the Kn increases, Beskok (see Karniadakis et al. 2005; Gad-el-Hak 1999 and the references cited therein) argued that higher order of the Kn and higher order derivatives of velocity must be used in the slip equations. For curved surface, Lockerby et al. (2004) accounted for the contribution of normal velocity in the viscous stress. In all the aforementioned studies, the gas molecules are not subject to any external forces before arriving at the wall, which is not applicable in the presence of volume force field such as gravity, electrostatics, etc. With these force fields, the slip velocity is different from flows driven by pressure gradient and cannot be simply described by (2). In what follows, on the basis of kinetic theory, we derive the new slip equation that accounts for the external body force field.

2 Slip model for micro/nano gas flows induced by body force

In the following derivation, the gas flow is assumed to be isothermal so that the influence of temperature on the slip velocity is not taken into account. Using the similar approach of Beskok (see Karniadakis et al. 2005), let us consider a control surface s near and parallel to the wall

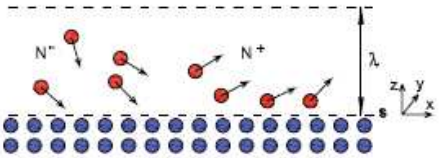


Fig. 1 Collision model between gas molecules and a solid wall. N^- and N^+ are respectively the number of molecules going downward and upward and passing through the surface s near the wall within one unit time. If there is no accumulation of gas near the wall, $N^- = N^+$

(see Fig. 1). For a unit time, there are N gas molecules passing through the surface which are composed of N^- molecules going downward and N^+ going upward with respective average tangential velocities, $<v_x^->$ and $<v_x^+>$. The gas average tangential velocity at the wall v_s may be written as

$$N^+ <v_x^+> + N^- <v_x^-> = N v_s \tag{6}$$

The molecules that go upward are those that previously went downward and were reflected at the surface s. Since the reflection is either diffusive or specular by the fractions σ_v and $1 - \sigma_v$, the following relation holds for a wall moving at velocity v_w:

$$N^+ <v_x^+> = (1 - \sigma_v) N^- <v_x^-> + \sigma_v N^- v_w \tag{7}$$

which is equivalent to

$$N v_s = N^- \left[<v_x^-> + (1 - \sigma_v) <v_x^-> + \sigma_v v_w \right] \tag{8}$$

Without external volume force, the N^- molecules colliding with the wall come from one mean free path λ away from the wall without collision so that their velocity does not change $<v_x^-> = v_\lambda$. We also assume that $N^- = N^+ = N/2$. It follows

$$2 v_s = [(2 - \sigma_v) v_\lambda + \sigma_v v_w] \tag{9}$$

The Taylor development of v_λ near the wall, $v_\lambda = v_s + \lambda \frac{\partial v}{\partial z}\big|_w$, gives the relation for slip velocity v_{slip} defined as $v_s - v_w$ (first-order Maxwell's relationship)

$$v_{slip} = \alpha \lambda \left. \frac{\partial v}{\partial z} \right|_w \quad \text{with} \quad \alpha = \frac{2 - \sigma_v}{\sigma_v} \tag{10}$$

In the presence of uniform volume force, i.e., in the case where a constant acceleration γ_x is applied on each gas molecule, $<v_x^->$ is no longer equal to v_λ. When impinging at the wall surface, the term $\gamma_x \beta <\tau>$ should be added to the average tangential velocity

$$<v_x^-> = v_\lambda + \gamma_x \beta <\tau> \tag{11}$$

where $<\tau>$ is the mean time for the molecules to arrive at the surface after the previous collision and is assumed to be $\lambda/\bar{c}$ where $\bar{c}$ is the thermal speed of the gas. For gases in local equilibrium, the thermal speed is estimated by $\bar{c} = \sqrt{2 k_B T/m}$. The constant β, introduced in the last term of (11), can be seen as a factor which accounts for the differences between the idealized conditions used to derive the slip model and the realistic ones. In reality, these differences can be due to the following reasons:

- the wall in the model is idealized as a surface and the gas wall collisions only take place at this surface. In fact, the wall also has an atomistic structure and the interaction force must be taken into account at distance of several molecular diameters.
- after arriving at the wall, the gas molecules can stay near the wall during a finite duration of time before leaving.

The value of β is expected to be close to unity. The slip equation with the corrected term becomes

$$v_{slip} = \alpha \lambda \left[\beta \frac{\gamma_x}{\bar{c}} + \left. \frac{\partial v}{\partial z} \right|_w \right] \tag{12}$$

Equation 12 is the new slip equation for general flows in which the body force is involved. In what follows, we study a particular case where the gas flow of viscosity, μ, is induced by a constant body force, $\rho \gamma_x$, along one direction x. Without pressure gradient, the velocity profile is given by

$$v(z) = \frac{\rho \gamma_x}{2\mu} \left(\frac{H^2}{4} - z^2 \right) + v_{slip}, \tag{13}$$

which when combined with the new slip model Eq. 12 yields the dimensionless form

$$\frac{\bar{c} v_{slip}}{\lambda \gamma_x} = \alpha \left[\beta + \frac{1}{\mu^* \mathrm{Kn}} \right], \quad \mu^* = \frac{\mu}{\bar{\mu}}. \tag{14}$$

In the above equation, μ^* is the scaled viscosity, and $\bar{\mu}$ is the kinetic theoretical viscosity (Liou and Fang 2003; Struchtrup 2005) defined as $\bar{\mu} = \frac{1}{2} \rho \lambda \bar{c}$. The dimensionless slip length L_s^* can be calculated accordingly:

$$L_s^* = \alpha \mathrm{Kn} [\beta \mu^* \mathrm{Kn} + 1] \quad \text{with} \quad L_s^* = L_s/H \tag{15}$$

We can deduce that the derived slip length is second-order dependent of the Kn. The influence of the volume force on the slip length becomes thus important when Kn is large enough. The ratio L_s^*/Kn is no longer equal to the constant α but is dependent on the channel characteristic dimension H via a composite parameter $(\mu^* \mathrm{Kn})^{-1}$. If Kn is increased and the variation of fluid viscosity μ is small, we shall observe an increase in the ratio L_s^*/Kn. In what follows, we use the molecular dynamics approach to valid this prediction and determine as well the two new model parameters α and β.

3 Molecular dynamics validation

In order to recover the dependence of slip velocities on the Kn and volume force, we simulate a flow induced by

uniform external volume force. The gas–solid couple investigated is helium (He) and copper (Cu). The choice of the couple He–Cu is motivated by two reasons: first, the accommodation coefficients derived experimentally and numerically are shown to be in good agreement (see for example ref. Finger et al. 2007) and, second the interaction potentials between these atomic species have been widely used (see ref. Foiles et al. 1986; Daw and Baskes 1984; Plimpton 1995; Finger et al. 2007; Allen and Tildesley 1989). However, the present method can be applied to any gas/wall system as long as the interaction potential between the atoms is properly provided. Since the slip length depends on what happens at the interface, the final results are strongly affected by the choice of the system.

The channel is made of two parallel solid walls, each of them containing nine layers (or 4 lattice units) of Cu atoms placed at fcc lattice sites. The lattice constant is chosen initially equal to 3.615 Å. The interaction forces between Cu atoms are derived from the EAM potential (Foiles et al. 1986; Daw and Baskes 1984)

$$V_i = F\left[\sum_j \rho_e(r_{ij})\right] + \frac{1}{2}\sum_{i\neq j}\phi(r_{ij}) \tag{16}$$

where V_i is the potential energy of atom, i, composed of the binary potential, $\phi(r_{ij})$, and embedded potential, F, accounting for electron density contribution, ρ_e. The interaction forces for the couples He–He and He–Cu are derived from the widely used Lennard–Jones potential

$$V_i = \sum_j 4\varepsilon\left[\left(\frac{\sigma}{r_{ij}}\right)^{12} - \left(\frac{\sigma}{r_{ij}}\right)^{6}\right] \tag{17}$$

The parameters used in this article are those from Allen and Tildesley (1989), Finger et al. (2007), $\varepsilon_{He-He} = 0.00088$ eV, $\sigma_{He-He} = 2.28$ Å, $\varepsilon_{He-Cu} = 0.0225$ eV, $\sigma_{He-Cu} = 2.29$ Å. The He–Cu parameters have been calculated using the Lorentz–Berthelot mixing laws from the He–He and Cu–Cu parameters in Allen and Tildesley (1989). The last atom layer at the two walls is fixed (see Fig. 2). The remaining atoms of the wall and the gas are maintained at the same temperature 120 K as usual by scaling method after removal of the mean velocity. On average, the wall is kept immobile, i.e $v_w = 0$.

In this study, the global number density of the gas is kept constant: $n = 0.0026$ Å^{-3} (or $\rho = 1.78 \times 10^{-14}$ pg/Å^3) while the channel height, H, and acceleration, γ_x, are varied to obtain results for different global Kn and volume forces, f. At the small density number and temperature of our simulations (e.g., 120 K), the helium is in gaseous phase. Three values of $H = 361$, 260, and 174 Å corresponding respectively to Kn = 0.046, 0.064, and 0.098 are considered. These three Kn numbers are chosen to fall into the range (0.01–0.1) in order to assure the slip flow regimes in our test cases according to Karniadakis et al. (2005). The two other dimensions of the simulation box along x-axis (the flow direction) and along y-axis denoted shortly by length L and width B are $L = H$ and $B = H/2$. For each channel height, the acceleration applied on each atom is varied as $\gamma_x = 0.0036, 0.012$, and 0.024 Å/ps^2. The computations are carried out by using LAMMPS, an open source parallelized code (Plimpton 1995) on an IBM Power6 machine. The equations of the particle motion are integrated using a Leapfrog-Verlet algorithm with a time step 0.002 ps. The steady state is achieved after 5×10^6 time steps, and it takes another 2×10^6 time steps for the average process. All the models are constructed in 3D with the parameters given in Table 1. Due to the high density of the solid wall, an important number of Cu atoms are considered. The largest model, case Kn = 0.046, involves 289,500 molecules and takes 8 h of computation on 512 processors.

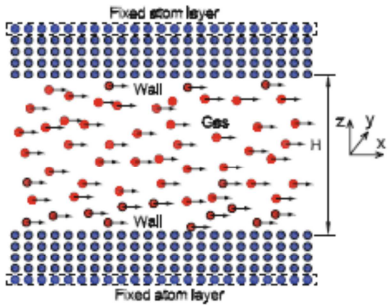


Fig. 2 One dimensional flow induced by external volume force. The simulation domain is periodic in directions x, y. The external volume force in direction x is produced by applying additional constant acceleration, γ_x, on each gas atoms

In order to obtain accurate solutions, the channel has been divided in a sufficiently large number of layers for the average procedure. For $\gamma_x = 0.012$ Å/ps^2 and different Kn, the velocity profiles in the upper half channel are plotted in Fig. 3. We find good agreement between analytical solution (Eq. 13) and the numerical results in the major part of the channel. The global viscosity of the fluid μ and slip velocity, v_{slip}, are obtained by fitting the numerical velocity profiles (Fig. 3) with Eq. 13, given in columns 3, 4 of Table 2. It is noted that the determination of μ is based the

Table 1 Size of the simulation box and number of helium and copper atoms for different Knudsen numbers

Kn	H (Å)	L (Å)	B (Å)	Cu atoms	He atoms
0.046	361	361	180	230,700	58,800
0.064	260	260	130	51,840	22,680
0.098	174	174	87	23,040	6,624

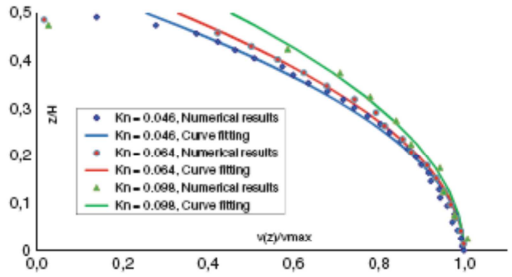


Fig. 3 Velocity profiles for the upper half of the channel obtained by MD simulation (*marker line*) and fitted by analytical formula (*solid line*). In the figure, the acceleration γ_x is kept constant at 0.012 Å/ps^2 while the Knudsen number is varied. The vertical and horizontal axis represent normalized coordinate, z/H and velocity, $v(z)/v_{\max}$, along the flow direction. The velocity $v_{\max}$ is the maximal velocity found in the middle of the channel

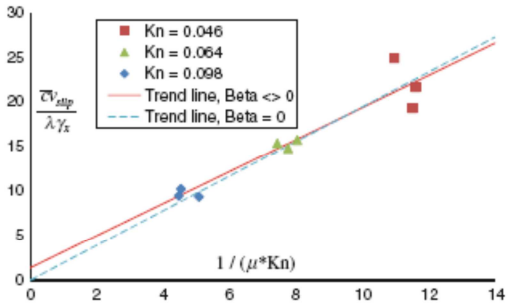


Fig. 4 Relations between two dimensionless quantities $\frac{\overline{c}v_{slip}}{\lambda\gamma_x}$ and $1/(\mathrm{Kn}\,\mu^*)$. The solid line represents the Eq. 14 which fits the numerical results. This line makes an angle arctan α with the horizontal axis and cuts the vertical axis at $\alpha\beta$. The dashed line represents (14) with $\beta = 0$ that fits the numerical results

Table 2 Numerical results from MD simulations

Kn	γ_x (Å/ps^2)	$\mu \times 10^5$ (Pa s)	v_{slip} (Å/ps)	$\frac{L_s^*}{\mathrm{Kn}}$	$\frac{1}{\mu^*\mathrm{Kn}}$	$\frac{\overline{c}v_{slip}}{\lambda\gamma_x}$
0.046	0.0036	1.89	0.18	1.87	11.60	21.80
	0.012	1.91	0.54	1.69	11.50	19.40
	0.024	2.00	1.38	2.20	11.30	25.00
0.064	0.0036	1.95	0.14	1.97	8.05	15.80
	0.012	2.02	0.43	1.91	7.77	14.90
	0.024	2.11	0.89	2.10	7.44	15.50
0.098	0.0036	2.03	0.08	1.90	5.08	9.41
	0.012	2.31	0.27	2.12	4.48	9.51
	0.024	2.27	1.38	2.26	4.54	10.03

curvature of the velocity profile and the average density, ρ, regardless of the redistribution of density at the steady state.

From the results reported in Table 2, it can be seen that L_s^*/Kn tends to increase with Kn. This trend cannot be accounted for by the usual one parameter model. In order to determine the two constants α and β in our proposed model (see Eq. 14), we plotted two dimensionless quantities $\frac{\overline{c}v_{slip}}{\lambda\gamma_x}$ and $(\mathrm{Kn}\mu^*)^{-1}$ from the last two columns of Table 2 into Fig. 4. We found the straight line that best fits these data. In the framework of our problem, the two values $\alpha = 1.81$ and $\beta = 0.76$ were determined. As expected, the value β is of order unity while α corresponds to an accommodation coefficient $\sigma_v = 0.71$ which is in the experimental range [0.66, 1.0] by Seidl, reported in the article of Finger et al. (2007) for the couple He–Cu. It is noted that the two bound limits 0.66 and 1.0 of TMAC correspond to the two extreme impinging at angles 70° and 10° of helium molecules at a copper wall in Seidl's experiments (see Table 3).

The impact of parameter β on slip velocity depends on the relative importance between the two terms β and $(\mathrm{Kn}\mu^*)^{-1}$. For large Kn, the role of coefficient β becomes important, e.g. up to 20% when $\mathrm{Kn} = 0.098$ while for small Kn, e.g. $\mathrm{Kn} = 0.046$, this effect is almost negligible (6%). In order to compare with the classical model that involves a single parameter α, the numerical results are also fitted with a line passing through origin, the dashed line in Fig. 4. The coefficient α predicted by the classical model takes the higher value $\alpha = 1.95$ and shows more discrepancies with respect to the simulation results.

4 Concluding remarks and discussion

A new slip model for flows with volume force has been introduced. Two parameters with physical meanings that relate slip velocity and velocity gradient at walls are suggested. The first one is the traditional TMAC, as in the widely used Maxwell model, while the second one accounts for the additional velocity that a molecule encompasses owing to the applied force before striking at a the solid surface. Molecular dynamics calculations applied on the He–Cu couple allowed to determine both TMAC and the new parameter β introduced in the present work. TMAC is found to be in good agreement with experimental data. In the v_{slip} expression, the effect of parameter β increases with Kn, i.e. when the limit of transitional flow is reached.

The present model is useful for the global analysis of flows without knowing the presence of the Knudsen layer. In our MD simulations, both higher density and slower motion of gas molecules are observed near the walls and cause deviation of the numerical velocity from the Navier–Stokes solution. Similar phenomenon was encountered and discussed in Cao et al. (2005) from molecular viewpoint.

Table 3 Seidl experimental data on the couple He–Cu (see Finger et al. 2007) where TMAC depends on the collision angle of the gas molecules

Angle	Seidl variability	Seidl lower TMAC value	Seidl upper TMAC value
10	0.100	0.86	1.06
20	0.080	0.81	0.97
30	0.065	0.77	0.90
40	0.050	0.73	0.83
50	0.040	0.71	0.79
60	0.030	0.69	0.75
70	0.020	0.66	0.70

In general, when a molecule reaches a surface, it does not bounce back immediately but is often trapped by the potential well. The molecule remains near the wall for some time, interacts with many other solid atoms before escaping. Accounting for the Knudsen layer should lead to more accurate results (see Lockerby et al. 2005; Lockerby and Reese 2008). A model involving body force as well as Knudsen layer may be expected in the near future.

Acknowledgments The authors acknowledge the French National Institute for Advances in Scientific Computations (IDRIS) for computational support of this project through grant No.i2009092205. We also wish to thank the reviewers for their helpful comments that help to improve the quality of this article.

References

Allen M, Tildesley D (1989) Computer Simulation of Liquids. Oxford University Press, Oxford

Arkilic E, Breuer K, Schmidt M (2001) Mass flow and tangential momentum accommodation in silicon micromachined channels. J Fluid Mech 437:29–43

Arya G, Chang HC, Maginn EJ (2003) Molecular simulations of Knudsen wall-slip: effect of wall morphology. Mol Simulat 29:697–709

Cao B, Min C, Guo Z, (2004) Application of 2DMD to gaseous microflows. Chin Sci Bull 49:1101–1105

Cao B, Chen M, Guo Z (2005) Temperature dependence of the tangential momentum accommodation coefficient for gases. Appl Phys Lett 86:091905

Cao B, Chen M, Guo Z (2006) Effect of surface roughness on gas flow in microchannels by molecular dynamics simulation. Int J Eng Sci 44:927–937

Colin S, Lalonde P, Caen R (2004) Validation of a second-order slip flow model in rectangular microchannels. Heat Transf Eng 25:23–30

Daw MS, Baskes MI (1984) Embedded-atom method: derivation and application to impurities, surfaces, and other defects in metals. Phys Rev B 29:6443–6453

Finger G, Kapat J, Bhattacharya A (2007) Molecular dynamics simulation of adsorbent layer effect on tangential momentum accommodation coefficient. J Fluid Eng-T Asme 129:31–39

Foiles SM, Baskes MI, Daw MS (1986) Embedded-atom-method functions for the fcc metals Cu, Ag, Au, Ni, Pd, Pt, and their alloys. Phys Rev B 33:7983–7991

Gad-el-Hak M (1999) The fluid mechanics of microdevices-the freeman scholar lecture. J Fluid Eng-T Asme 121:5–33

Karniadakis G, Beskok A, Aluru N (2005) Microflows and nanoflows: fundamentals and simulation. Springer, New York

Liou W, Fang Y (2003) Microfluid mechanics. McGraw-Hill, New York

Lockerby DA, Reese JM (2008) On the modelling of isothermal gas flows at the microscale. J Fluid Mech 604:235–261

Lockerby DA, Reese JM, Emerson DR, Barber RW (2004) Velocity boundary condition at solid walls in rarefied gas calculations. Phys Rev E 70:017303

Lockerby DA, Reese JM, Gallis MA (2005) The usefulness of higher-order constitutive relations for describing the Knudsen layer. Phys Fluids 17:100609

Maali A, Bhushan B (2008) Slip-length measurement of confined air flow using dynamic atomic force microscopy. Phys Rev E 78:027302

Maxwell J (1879) On stresses in rarified gases arising from inequalities of temperature. Philos T Roy Soc A 170:231–256

Plimpton S (1995) Fast parallel algorithms for short-range molecular dynamics. J Comput Phys 117:1–19

Struchtrup H (2005) Macroscopic transport equations for rarefied gas flows: approximation methods in kinetic theory. Springer, New York